

A CAD integrated modular method of analysis of shear walls under earthquakes

C.M. Guo
Beijing Polytechnic University, People's Republic of China

A.A. Mufti
Computer Aided Design Centre, Technical University of Nova Scotia, Halifax, Canada

L.G. Jaeger
Research, Technical University of Nova Scotia, Halifax, Canada

ABSTRACT: This study expands upon previously reported work (Zhiming, 1986) and presents a non-linear finite element model for planar RC shear walls and a CAD integrated modular method for their analysis under seismic loads. The material properties are represented by elasto-plastic relationships in which yielding, plasticity, crack opening and closing and crushing of the concrete are taken into account as well as yielding of the steel reinforcement. The method is programmed and applied to several numerical examples. Comparisons with experimental data are presented.

1 INTRODUCTION

Reinforced concrete shear walls play a very important role in providing the necessary strength and stiffness to a building which is subjected to seismic loading. The necessity for safe and economical design of such structures makes a strong case for carrying out research in order to assess realistically their behaviour during earthquakes. Since the behaviour of the structure during the earthquake is significantly non-linear and the seismic loading involves many reversals of direction of load, the eventual structural condition of the shear wall is path-dependent. In particular it may not be possible in all cases to estimate the collapse behaviour of the structure on the basis of monotonically increasing loads. One approach is to predict the non-linear response of the RC structure to a particular earthquake excitation using the finite element method (Penzien, 1975). A number of papers have been devoted to the subject over the past twenty years (Nilson, 1965; Franklin, 1970; Cervenka, 1970; Yuzugullu, 1972; Darwin, 1974 and Hsu, 1974). The purpose of this paper is to show a preferred application of the finite element method to the analysis of shear walls under earthquake loading. The method uses CAD integrated modules and is sufficiently cheap that a large number of different excitations can be used. Thus, although any one particular solution may not give generic information, consideration of several such solutions together can give

valuable insights.

2 MATERIAL IDEALIZATION

A material model has been developed and is summarized below. It may be noted that the model has three main attributes (a) plain concrete stress-strain properties in biaxial compression (b) deformation of the cracked concrete element (c) stress-strain properties of the steel reinforcement.

2.1 Constitutive relationships

For the failure of concrete in tension a maximum normal stress theory has been used, and for the failure of concrete in compression a maximum strain theory has been adopted. The assumed failure envelopes for concrete in a biaxial state of stress and strain are those of Agrawal (1977) and are shown in Figure 1. The yielding is governed by a yield criterion of the form:

$$F(\{\sigma\}^c) = 0 \quad (1)$$

In accordance with the Von-Mises yield criterion, the yield surface is defined as:

$$F(\{\sigma\}^c) = \left[(\sigma_x^c)^2 - \sigma_x^c \sigma_y^c + (\sigma_y^c)^2 + 3(\sigma_{xy}^c)^2 \right]^{1/2} - \sigma_0^c \quad (2)$$

It has been suggested that the elasto-plastic matrix takes the form:

$$[D_e]_{ep}^c = [D_e]^c - [D_e]^c \left\{ \frac{\partial F}{\partial \{\sigma\}} \right\} \left\{ \frac{\partial F}{\partial \{\sigma\}} \right\}^T$$

$$[D_e]^c \left[\left\{ \frac{\partial F}{\partial \{\sigma\}} \right\} [D_e]^c \left\{ \frac{\partial F}{\partial \{\sigma\}} \right\} \right]^{-1} \quad (6)$$

where $[D_e]^c$ = the elastic material matrix of uncracked concrete of element given by equation (7).

$$[D_e]^c = \frac{E_c}{(1-\nu_c^2)} \begin{bmatrix} 1 & \nu_c & 0 \\ \nu_c & 1 & 0 \\ 0 & 0 & \frac{(1-\nu_c)}{2} \end{bmatrix} \quad (7)$$

$$\left\{ \frac{\partial F}{\partial \{\sigma\}} \right\} = \frac{1}{\sigma_0^c} \{ (\sigma_x^c - 0.5\sigma_y^c), (\sigma_y^c - 0.5\sigma_x^c), 3\sigma_{xy}^c \}^T \quad (8)$$

The quantity σ_0^c is the uniaxial stress at yield. Concrete having one set of open cracks will start yielding in uniaxial compression if $\sigma_u^c \geq \sigma_c^c$. In this case, such a concrete is assumed to have been crushed if the uniaxial strain attains a certain value (often taken as 0.003).

The elasto-plastic matrix $[D_e]_{ep}^c$ takes the place of the elasticity matrix $[D_e]^c$ in incremental analysis if the concrete becomes elasto-plastic.

2.4 Opening, closing and reopening of cracks in concrete

Referring to Figure 3, the concrete cracks for the first time when a principal stress equals or exceeds the allowable tensile stress. A set of cracks is formed in an element perpendicular to the direction of the principal tensile stress, if $\sigma_u^c \geq \sigma_t^c$. The cracked concrete is assumed to behave as a uniaxial material and carries stresses σ_u^c in the direction of cracks. This rule is also suitable for the second set of orthogonal cracks. After these cracks have been formed, the cracked concrete is allowed to retain some shear stiffness and is capable of transferring shears.

A set of open cracks is assumed to have been re-closed if

$$\text{or} \quad = \left[(\sigma_1^c)^2 - \sigma_1^c \sigma_2^c + (\sigma_2^c)^2 \right]^{1/2} - \sigma_0^c \quad (3)$$

where σ_0^c = uniaxial yield stress of concrete
 σ_1^c, σ_2^c = the principal stresses of concrete

Under biaxial compression, plain concrete starts yielding if $F(\{\sigma\}^c) > 0$. The concrete can sustain compression up to a certain limit beyond which it is crushed. The equivalent uniaxial strain for concrete under biaxial compression is determined as:

$$\epsilon_n = \left[(\epsilon_x^c)^2 - \epsilon_x^c \epsilon_y^c + (\epsilon_y^c)^2 + 0.75 (\epsilon_{xy}^c)^2 \right]^{1/2} \quad (4)$$

$$\text{or} = \left[(\epsilon_1^c)^2 - \epsilon_1^c \epsilon_2^c + (\epsilon_2^c)^2 \right]^{1/2} \quad (5)$$

where $\epsilon_1^c, \epsilon_2^c$ = the principal strains for concrete
 ϵ_n = equivalent uniaxial strain

Hilsdorf, Kupfer and Rusch (1969) have indicated that the biaxial tensile strength of concrete is almost equal to its uniaxial tensile strength. However, the concrete can withstand tensile stress up to a limit σ_t^c after which it cracks. The splitting stress σ_t^c is assumed to be the maximum principal tensile stress that can be attained before cracking of the concrete within an element.

2.2 Crack modes

To simulate the behavior of reinforced concrete under reversed loading, six crack modes for an element of concrete are allowed in the analytical model (Yuzugullu, 1972 and Darwin, 1974). These are shown in Figure 2.

2.3 Biaxial yielding of concrete

Based on the "Initial Stress Approach" (Zienkiewicz, 1969), uncracked concrete and concrete having all cracks closed is in a state of biaxial stress, and such a concrete starts yielding in biaxial compression if $F(\{\sigma\}^c) > 0$.

$$\epsilon_v < \epsilon_v^c \quad (9)$$

where ϵ_v = the strain normal to the cracks, as given by the expression:

$$\epsilon_v = \epsilon_x \sin^2 \alpha + \epsilon_y \cos^2 \alpha - \epsilon_{xy} \sin \alpha \cos \alpha \quad (10)$$

$$\epsilon_v^c = -\frac{\nu_c \sigma_u^c}{E_c} \quad (11)$$

where ν_c = Poisson's ratio of concrete

A set of closed cracks will reopen if $\sigma_v^c > 0$

where σ_v^c = the stress normal to the cracks. The form is as follows:

$$\sigma_v^c = \sigma_x^c \sin^2 \alpha + \sigma_y^c \cos^2 \alpha - 2\sigma_{xy}^c \sin \alpha \cos \alpha \quad (12)$$

2.5 Steel reinforcement

The steel reinforcement is assumed to be in a state of uniaxial stress. The bilinear stress-strain law is used. In our study, it is treated as a linear-elastic/perfectly plastic material.

2.6 Composite material property matrix

A "smeared" composite material property matrix is generated by adding the constitutive matrix for steel reinforcement to that of plain concrete. This can be written as:

$$[D_e] = [D_e]^c + [D_e]^s \quad (13)$$

Depending upon the state of plain concrete in an element, the elastic, yielded, cracked, or crushed state is utilized to represent $[D_e]^c$, respectively. The formulation of the matrix $[D_e]$ and the procedure of incorporating the yielding of steel reinforcement is described below.

3 FINITE ELEMENT MODEL

For the purpose of this study, the rectangular plane stress element with three degrees of freedom at each node, based on the work of Sisodiya, Cheung and Ghali (1972) is used and shown in Figure 4. The degrees of freedom of each node are the translations 'U' and 'V' in X and Y direction, respectively, and the inplane

rotation ' θ_x ' of the node. The minimum potential energy theorem is used in the familiar way.

Complete details of the element formulation are given in Agrawal (1977).

4 SOLUTION PROCEDURE

The nonlinear analysis of the RC planar structure under ground motion is conducted through the use of an iterative procedure. The structure response is computed by applying the ground motion in a sequence of incremental load steps. Within each step, the nonlinear equilibrium equations are linearized using a stiffness approach, i.e.

$$[K_T] \{\Delta\delta\} = \{\Delta P\} \quad (14)$$

where $[K_T]$ is a stiffness matrix which is updated at the end of each iterative step, and thus reflects the current state of material properties of the structure. These equations are solved to determine increments of nodal displacements.

5 NUMERICAL RESULTS AND COMPARISONS

Numerical examples are given below of the behavior of two shear walls using the proposed analytical model. The material properties of chosen test specimen are those of Lybas (1977) and Hsu (1974), respectively. The idealizations of shear wall are shown in Figure 5. Tables 1 and 2 give comparison of natural frequency and response values. Figures 6 and 7 show the crack patterns. The agreement with the experimental results obtained by Lybas and Hsu is in general quite good.

6 CAD INTEGRATED MODULES

Although the computational efficiencies of general finite element programs have increased steadily over the past few years, the time-consuming process of accurate data presentation is still a burden for most users of the finite element method. In practice, using conventional methods, approximately ninety percent of the total time of analysis may be consumed by input and output. Clearly, there is a need for improved pre- and post-processing procedures to parallel the advances made in computational techniques. The achievement of such improved procedures will have the additional benefit that because the user will need to concentrate on only minimal input data the occurrence of human errors in the pre-processing and post-processing

of data can be expected to diminish greatly.

Automated pre-processor and post-processor programs have been developed to help meet this need. These programs are supported by a computer graphics package called "UNIPLLOT" on the Cyber system. The color terminal Tektronix 41XX and Zeta multi-pen plotter are used to present both modelling and the results of analysis. The software automatically translates the graphically defined geometric data into the numerical description needed as input to the finite element analysis program. Also, the large amount of output from the analysis program is formulated into a picture file.

The three integrated CAD modules are pre-processor, analysis and post-processor.

6.1 Pre-processor

The pre-processor includes the geometric description and specification of the problem, and handles such specific attributes as element types, material properties and boundary conditions. Figure 5, which was produced by computer graphics, shows the modelling of two structures, i.e. Wall-1 and Wall-2.

6.2 Analysis

The analysis program is specific to non-linear finite element analysis of RC shear walls under earthquakes. The data is fed from the pre-processor and the analysis software provides the results such as stresses, displacements etc. to the post-processor. The total analysis procedure takes about 190 CPU seconds to complete 37 step iterations; at a cost of 10¢ per CPU second on the Cyber 825, total cost of the analysis is thus \$19 (Canadian funds).

6.3 Post-processor

The post-processor program is used to display structural idealization, deflections and stress contours. Figure 8 shows the structure deflections for Wall-1, magnified fifty times. Figures 9, 10 and 11 show the stress contours at two stages of the iteration process. The first stage is at 1st-27th step of iteration, at which point no cracks were present, i.e. all of the structural elements were still in the elastic state. The full structure stress contour clearly displays the stress concentration areas near the corner of the

window of the wall.

The second stage is at the 28-36th step of iteration, where now the structure has gone into a cracked and yielded state. The significant difference in the stress contours at the two stages may be noted. The progressively more non-linear behavior can be clearly seen from the displays.

In Table 3, computer time needed to create and display typical behavior is shown.

6.4 Concluding comments on the CAD modules

The utilization of CAD techniques has already proven to be of great advantage in understanding complex structural behavior and in the design of structures.

Integrated modules are being developed for dynamic display capability; these are expected to prove very useful to designers when carrying out non-linear dynamic structural analysis.

7 FURTHER DEVELOPMENT OF THE METHOD

The method as reported in this paper is still being refined and improved. In particular, if the input ground motion is very strong indeed, so that a large number of elements become yielded, cracked or crushed in a single load increment step, it is possible for the diagonal term of the stiffness matrix to become zero, i.e. for the stiffness matrix to become singular. This means of course that the calculation cannot continue. Work is now going on to develop a revised algorithm capable of coping with this condition.

REFERENCES

- Agrawal, A.W. 1977. Nonlinear analysis of reinforced concrete planar structures subject to monotonic, reversed cyclic and dynamic loads. Ph.D. Thesis, University of New Brunswick.
- Cervenka, V. 1970. Inelastic finite element analysis of reinforced concrete panels under inplane loads. Ph.D. Thesis, University of Colorado.
- Darwin, D. and Pecknold, D.A. 1974. Inelastic model for cyclic biaxial loading of reinforced concrete. Civil Engineering Studies, SRS No. 409, University of Illinois, Urbana, Illinois.
- Franklin, H.A. 1970. Nonlinear analysis of reinforced concrete frame and panels.

Ph.D. Thesis, University of California, Berkeley, California.

Hsu, L. 1974. Behavior of multistory reinforced concrete walls during earthquake. Ph.D. Thesis, University of Illinois.

Kupfer, H., Hilsdorf, H.K. and Rusch, H. 1969. Behavior of concrete under biaxial stresses. Journal ACI 66, No. 8: 656-666.

Lybas, J.M. and Sozen, M.A. 1977. Effect of strength and stiffness on dynamic behavior of reinforced concrete coupled walls. Civil Engineering Studies, SRS No. 444, University of Illinois.

Nilson, A.H. 1965. Nonlinear analysis of reinforced concrete by the finite element method. Journal ACI 65, No. 9: 757-766.

Penzien, J. 1975. Predicting the performance of structures in regions of high seismicity. Second Canadian Conference on Earthquake Engineering, Hamilton, Ontario.

Sisodiya, R.G., Cheung, Y.K. and Ghali, A. 1972. New finite elements with

applications to box girder bridges. Proceedings of the Institution of Civil Engineering, U.K. Supplement, Paper No. 747s, London: 207-225.

Yuzugullu, O. and Schnobrich, W.C. 1972. Finite element approach for the prediction of inelastic behavior of shear-wall frame systems. Civil Engineering Studies, SRS No. 386, University of Illinois.

Zhiming, L., Mufti, A.A. and Jaeger, L.G. 1986. Non-linear finite element analysis of shear walls under earthquakes. Proceedings of the 8th European Conference on Earthquake Engineering, Vol. 6.5, Lisbon: 25-32.

Zienkiewicz, O.C., Valliappan, S. and King, I.P. 1969. Elastoplastic solutions of engineering problems, 'initial stress' finite element approach. International Journal for Numerical Methods in Engineering 1: 75-100.

Table 1. Response frequency (Hz)

Example Shear Walls	Observed Values		Analytical Values	
	Pre-Test	Post-Test	Initial	End
Wall-1 (D-1)	12.0	4.7	13.294	4.361
Wall-2 (D-4)	8.5	5.5	11.839	5.260

Table 2. Comparison of response values

	Example Shear Walls			
	Wall 1 (D-1)		Wall 2 (D-4)	
	Analytical	Observed	Analytical	Observed
Time Duration	3.0	30.0	3.0	30.0
Base Acc. (G)	0.323	0.50	0.323	1.05
Base Shear (kip)	1.813	1.780	4.03	4.00
Base Moment (kip-in)	72.5	68.0	154.4	163.0

Note: 1 kip = 4.45 KN; 1 kip-in = 0.113 KN-M

Table 3. CPU time for the diagram

Diagram	CPU Time	Example
Structure Idealization	1.991 sec.	Figure 5
Deflection of Structure	2.131 sec.	Figure 8
Stress Contour	31.581 sec.	Figure 9

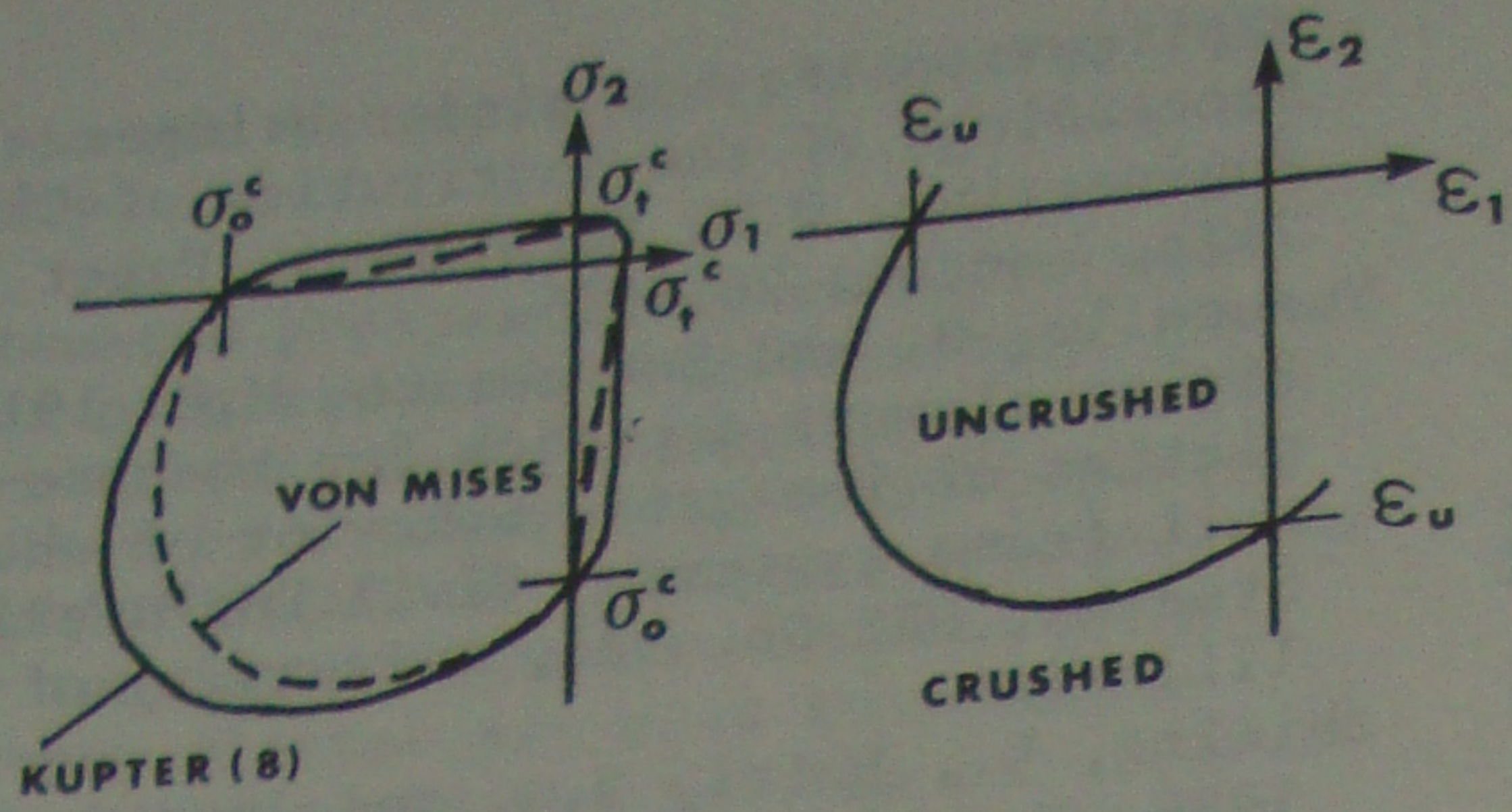


FIG. 1. YIELD SURFACE FOR CONCRETE.

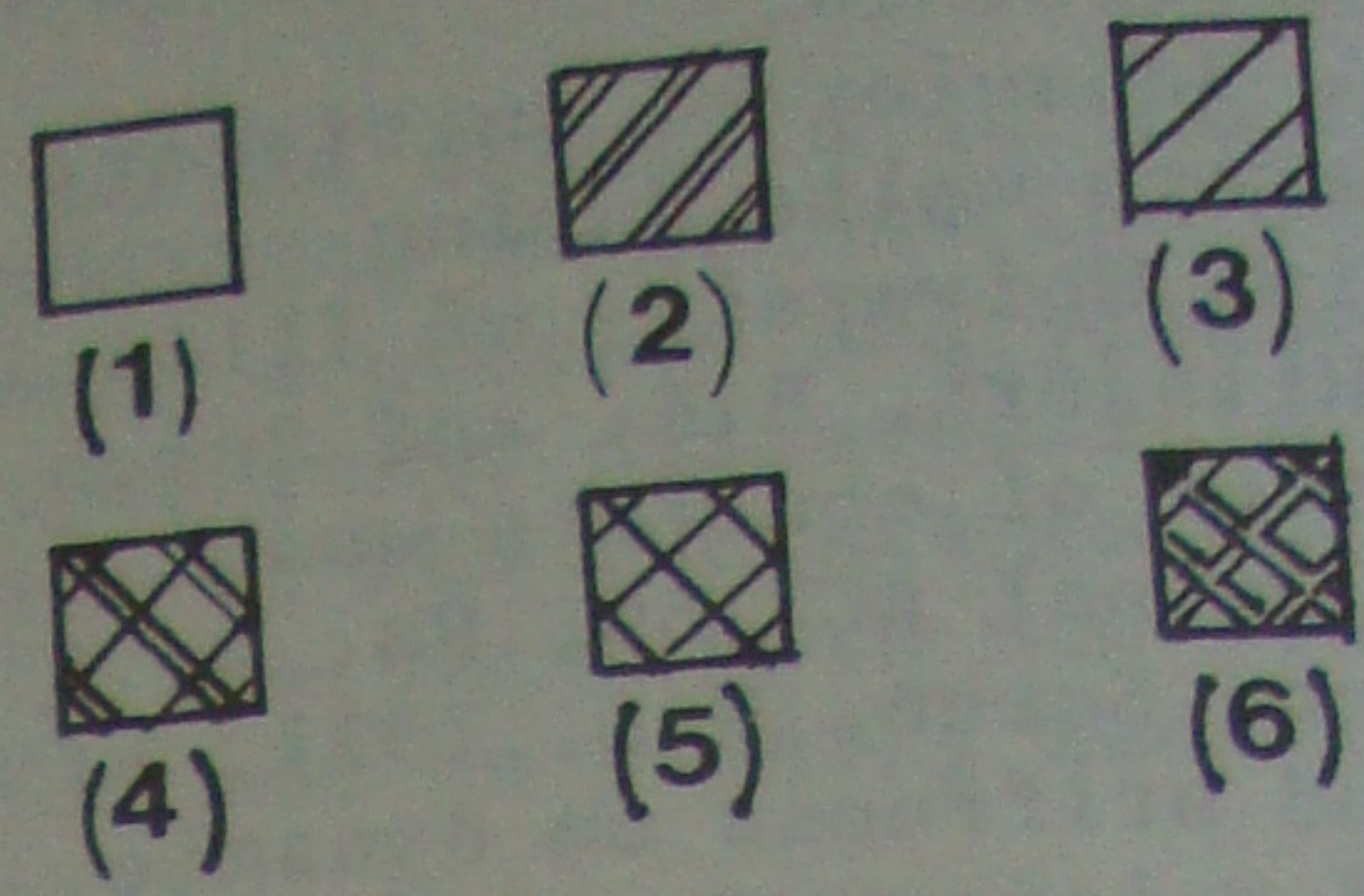


FIG. 2. CRACK MODES.

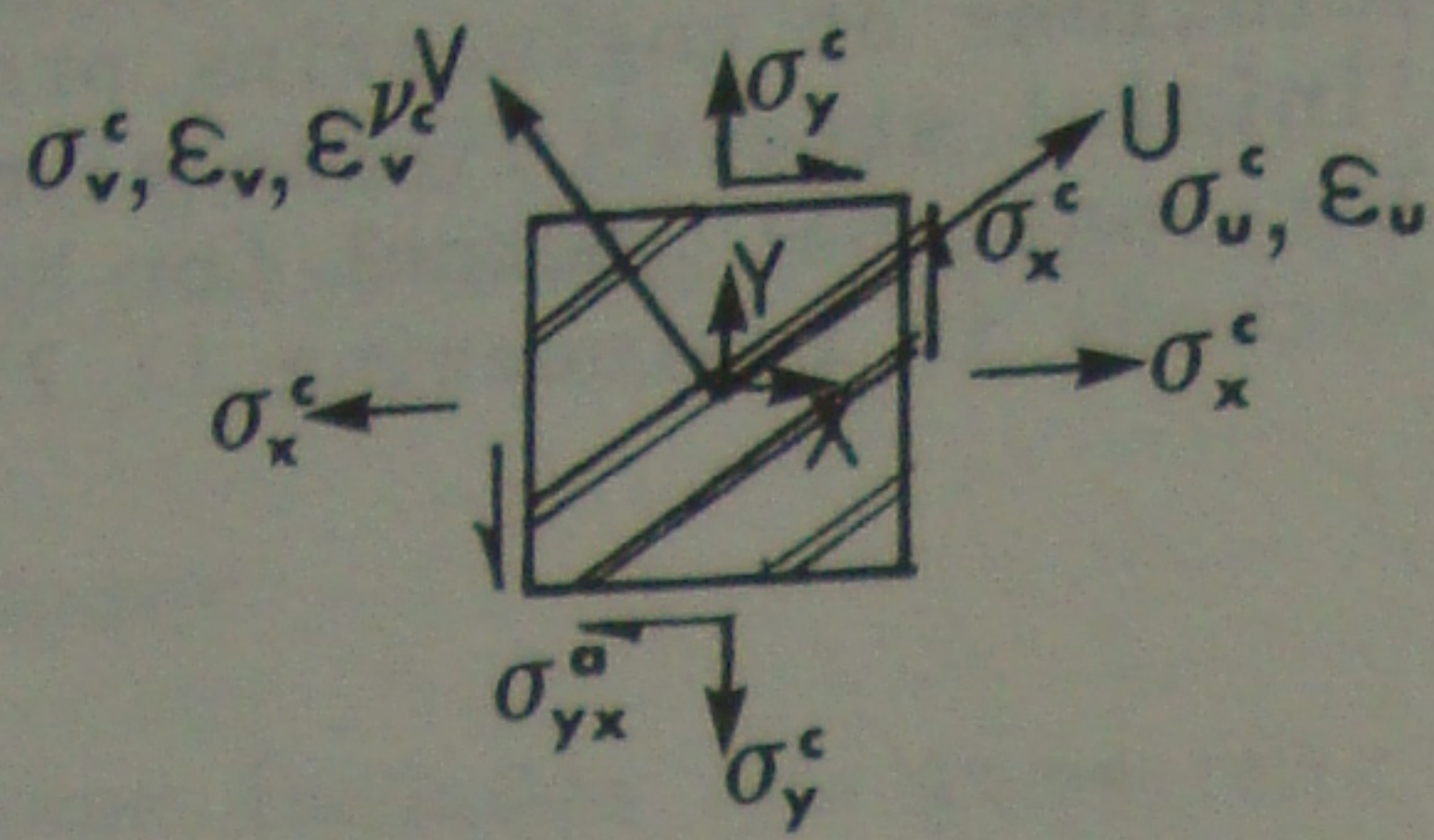


FIG. 3. CRACKED ELEMENT.

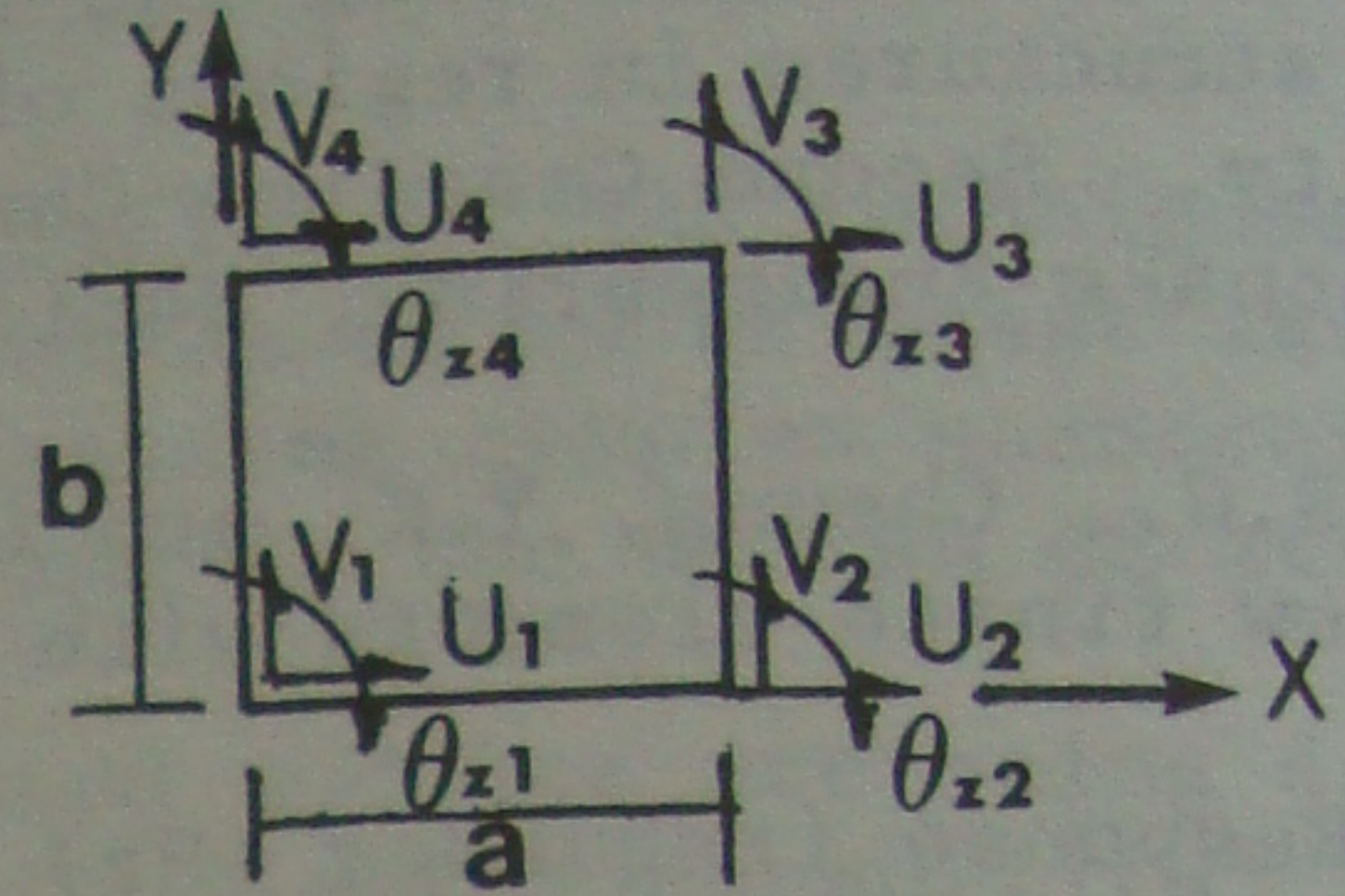


FIG. 4. RECTANGULAR PLANE STRESS ELEMENT.

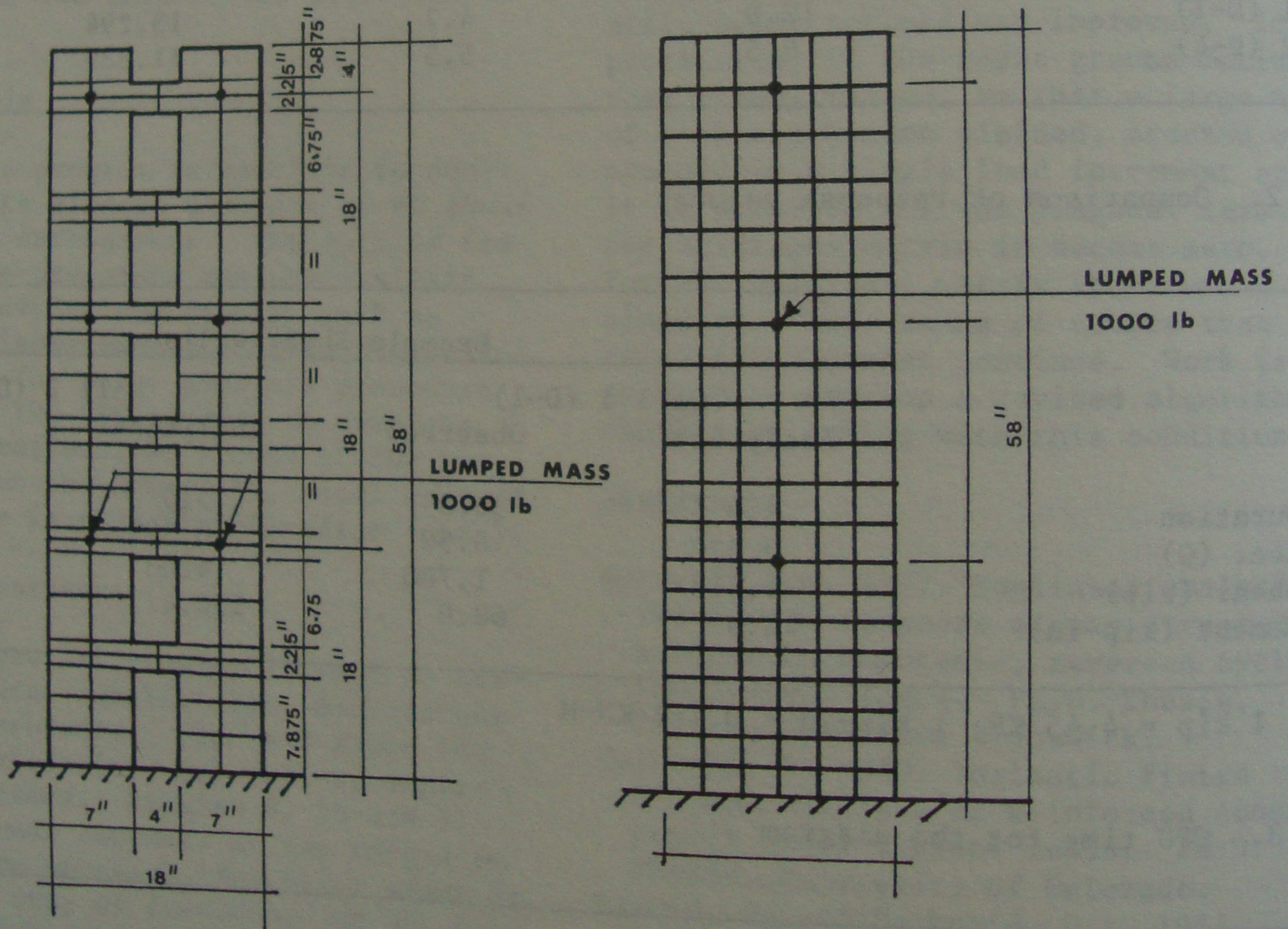
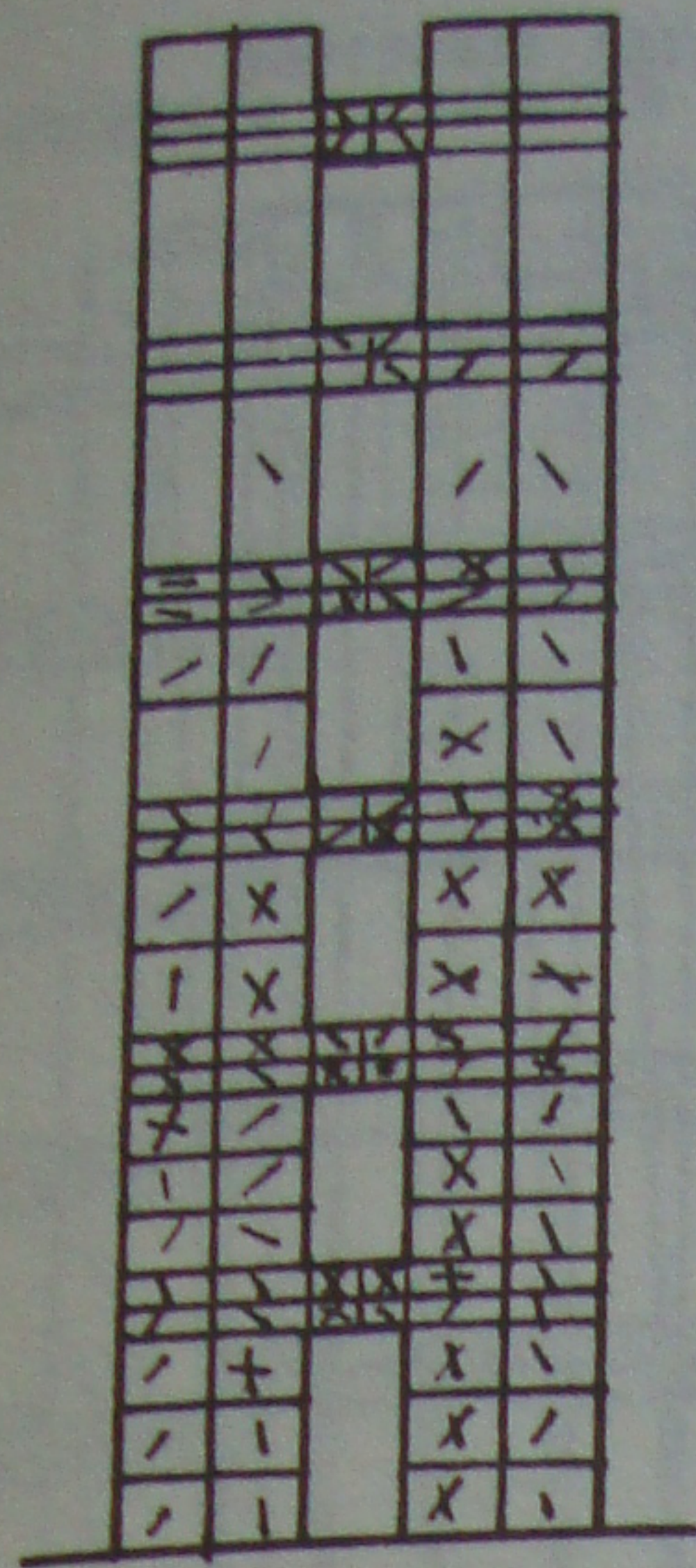
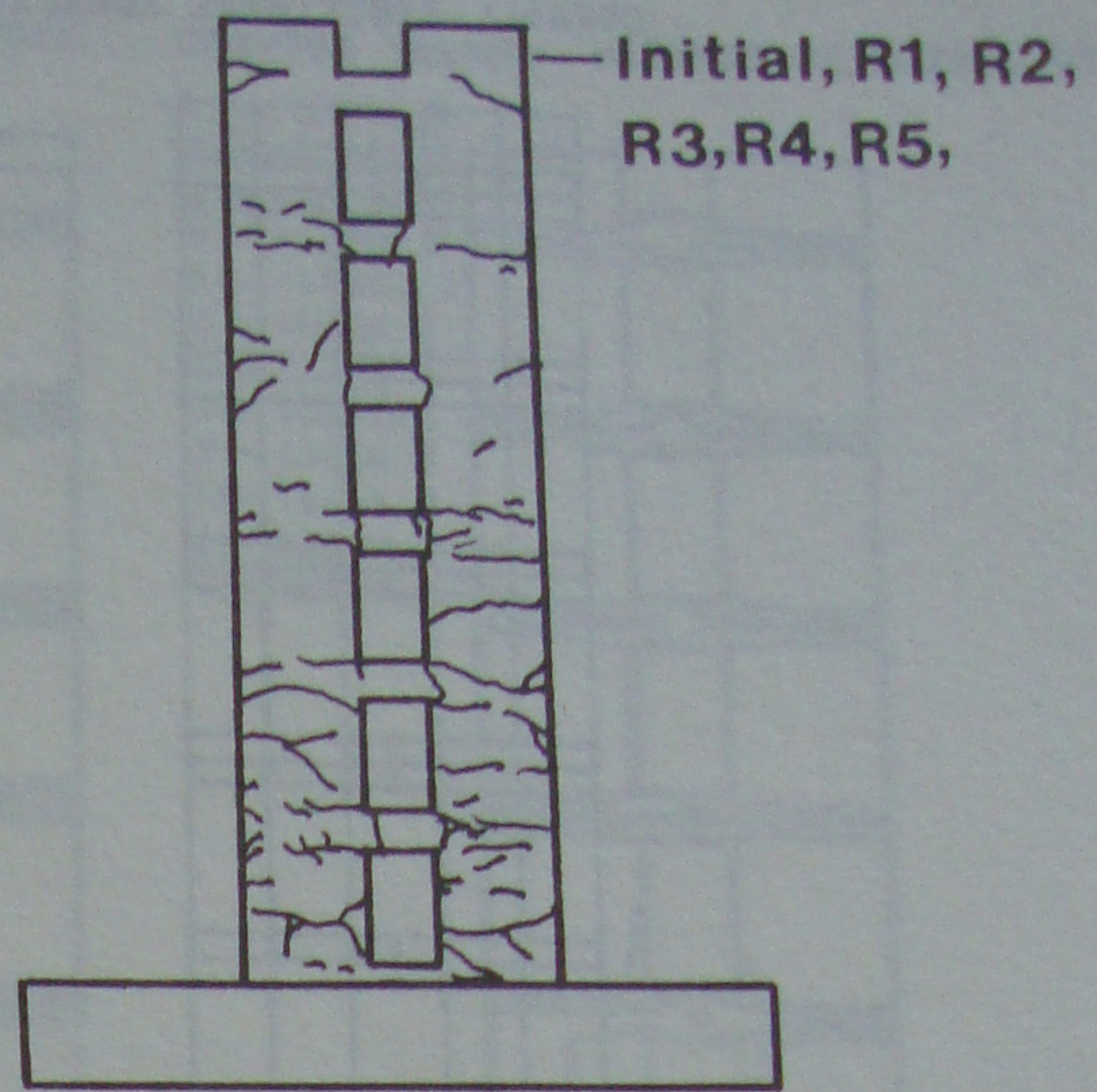


FIG. 5. SHEAR WALL IDEALIZATION USED IN THE EXAMPLE.

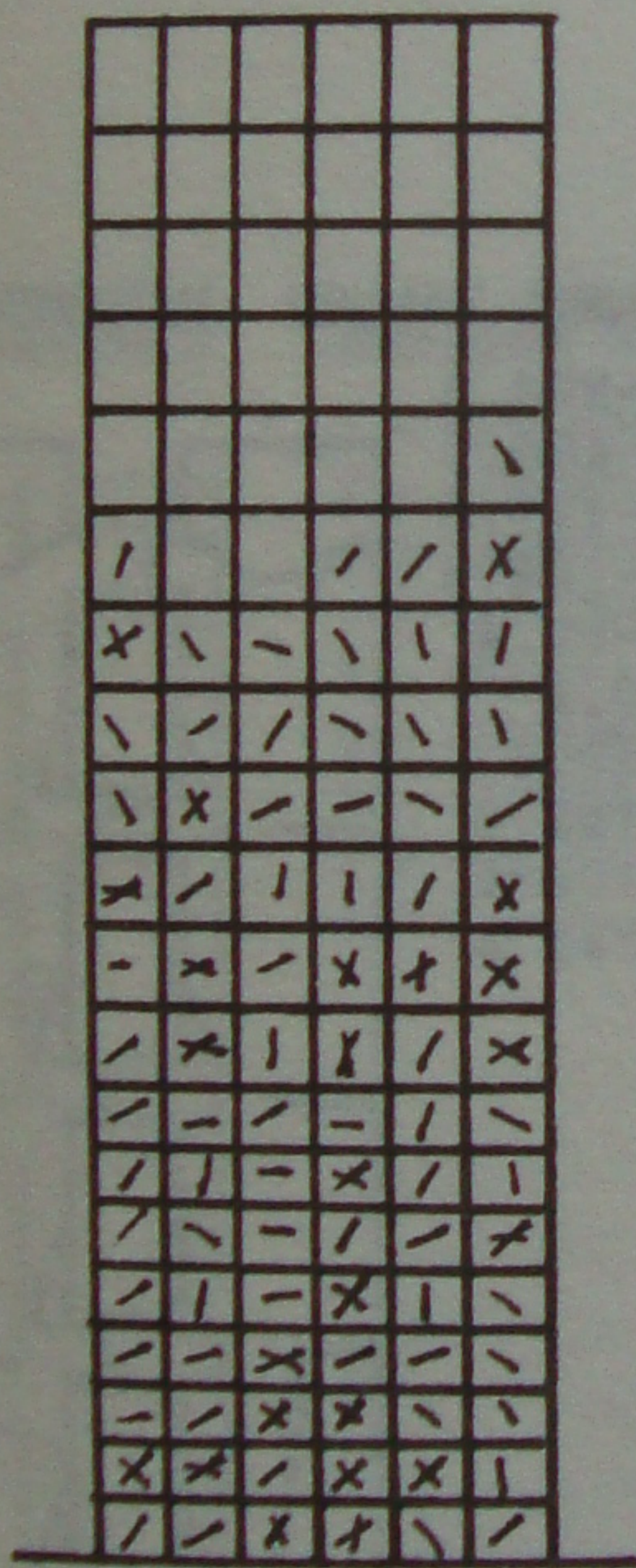


(A) ANALYTICAL

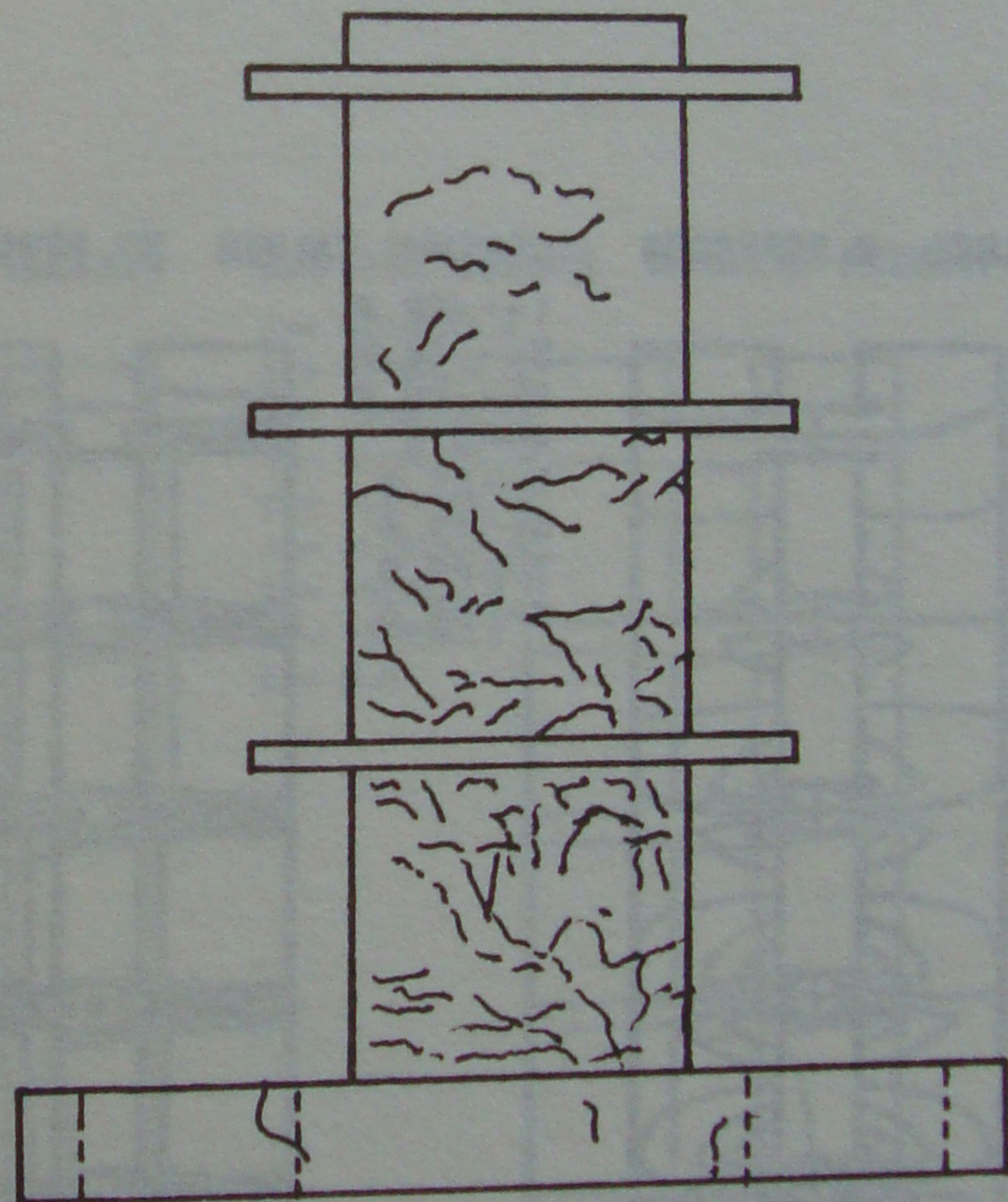


(B) OBSERVED Sozen (1977)

FIG.6. CRACKS PATTERN FOR SHEAR WALL - 1.



(A) ANALYTICAL



(B) OBSERVED Hsu (1974)

FIG.7. CRACKS PATTERN FOR SHEAR WALL - 2.

OVERALL STRUCTURAL IDEALIZATION DEFLECTED STRUCTURE

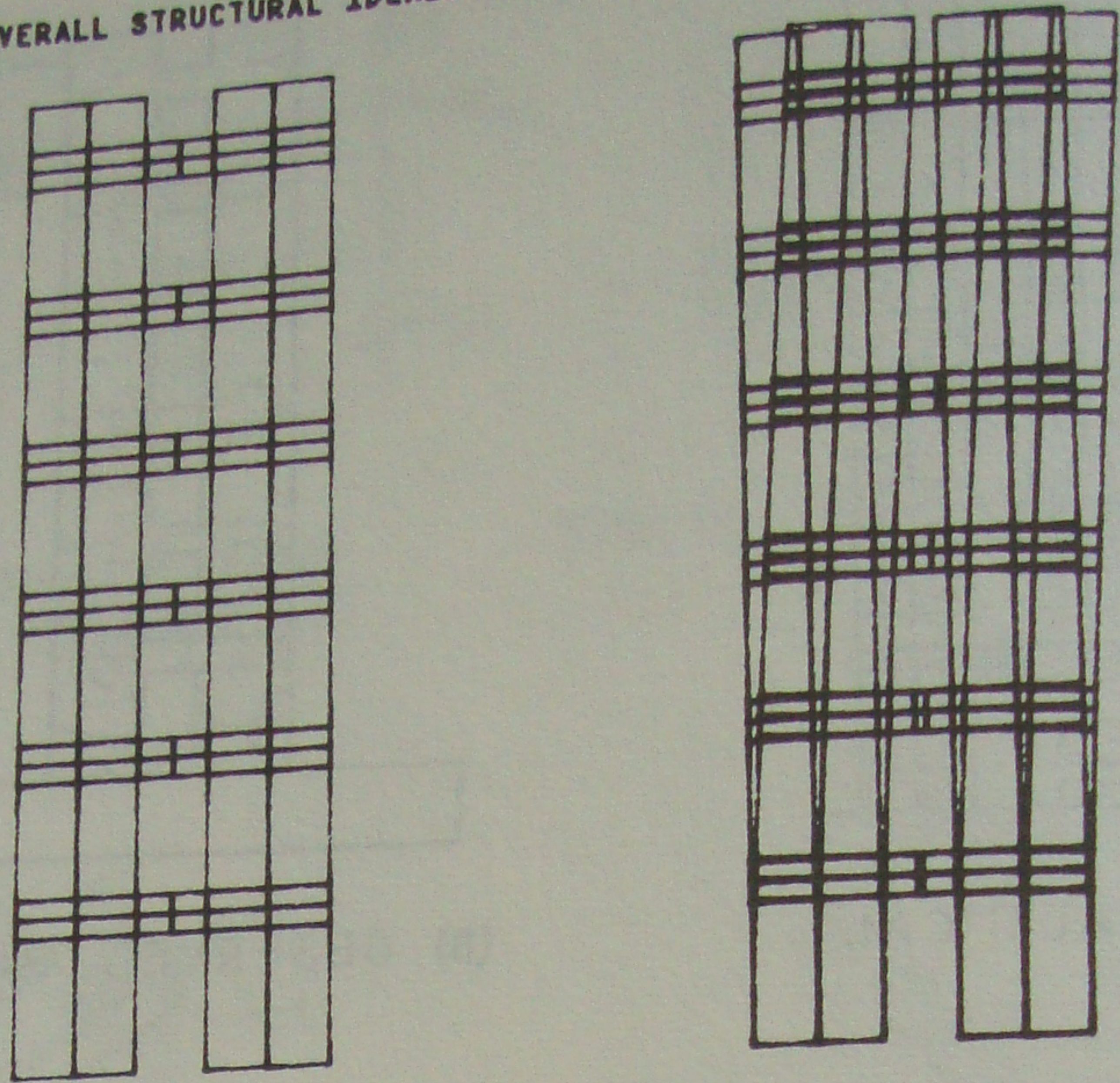


Fig. 8 WALL-1 at the 24th step of iteration

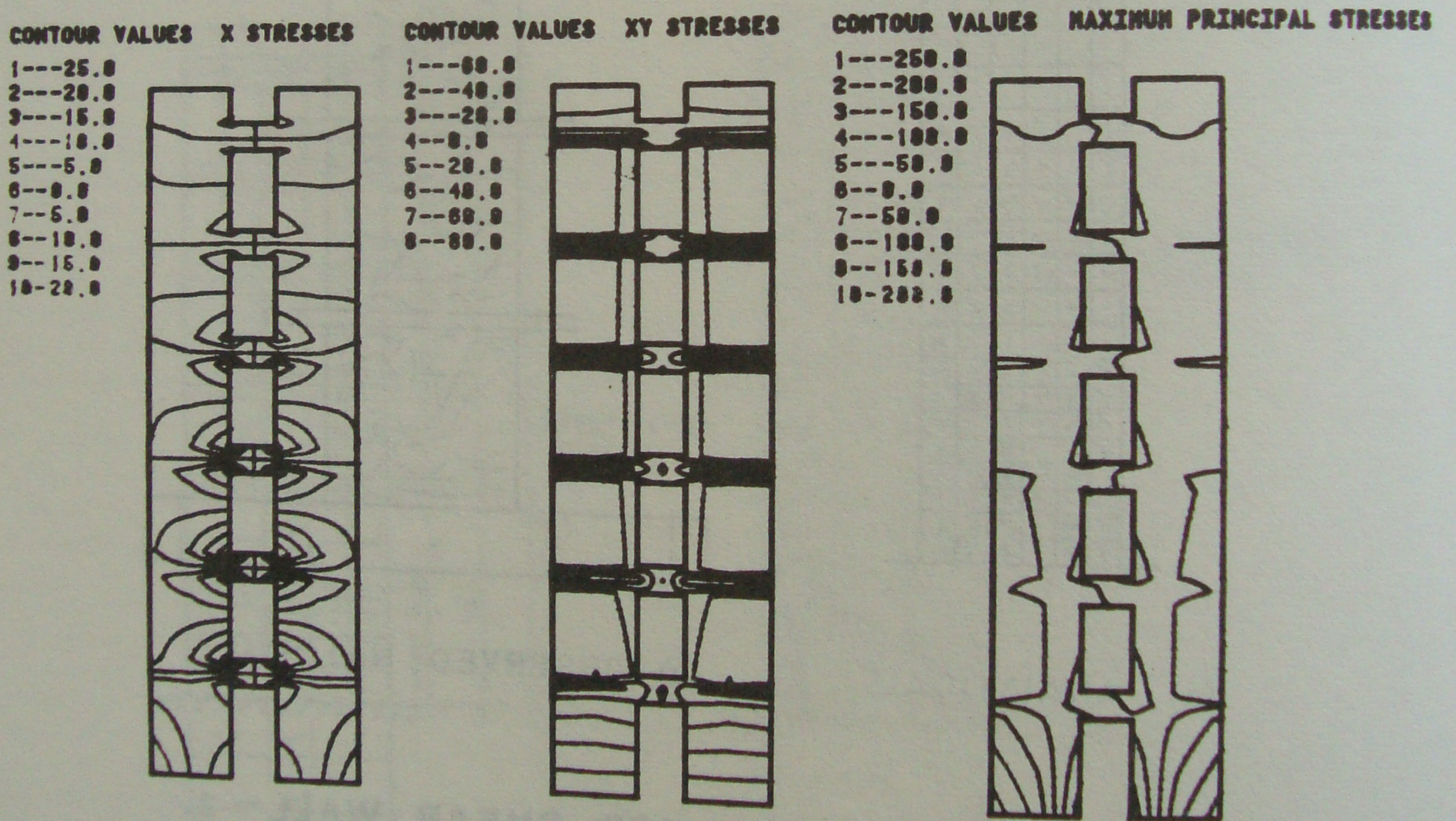


Fig. 9 WALL-1 at the 24th step of iteration

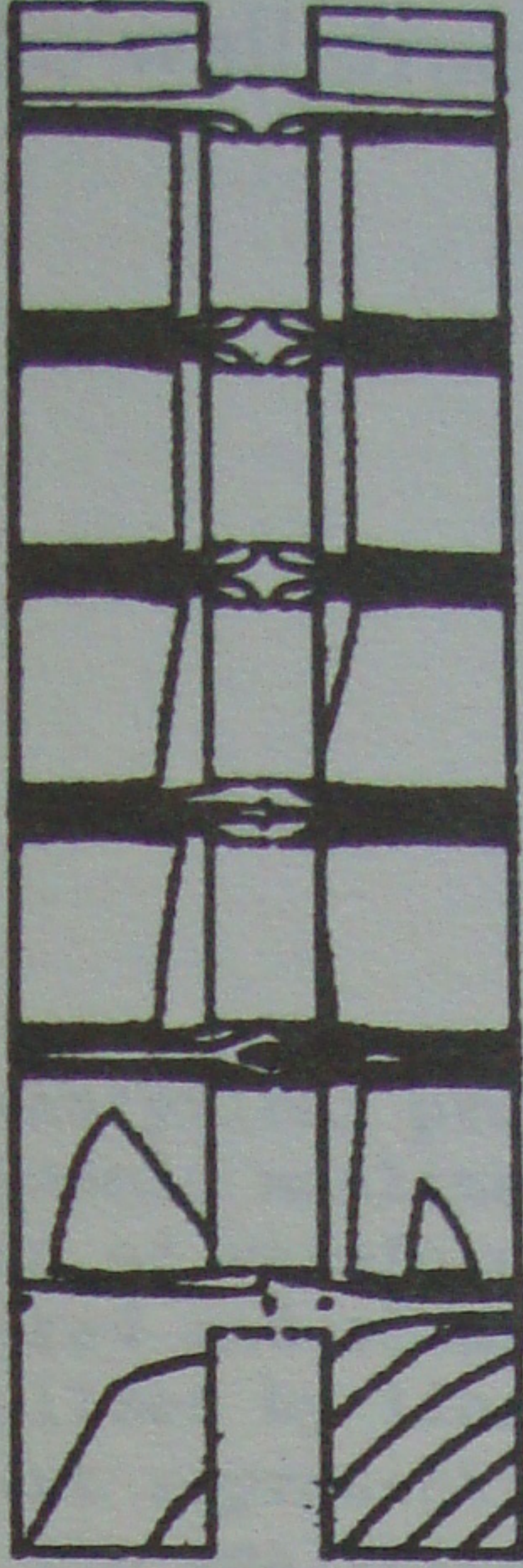
CONTOUR VALUES X STRESSES

- 1-- -6000.0
- 2-- -5000.0
- 3-- -4000.0
- 4-- -3000.0
- 5-- -2000.0
- 6-- -1000.0
- 7-- 0.0
- 8-- 1000.0
- 9-- 2000.0
- 10-- 3000.0
- 11-- 4000.0



CONTOUR VALUES XY STRESSES

- 1-- -7000.0
- 2-- -5000.0
- 3-- -3000.0
- 4-- -1000.0
- 5-- 1000.0
- 6-- 3000.0
- 7-- 5000.0
- 8-- 7000.0
- 9-- 9000.0
- 10-- 11000.0



CONTOUR VALUES MAXIMUM PRINCIPAL STRESSES

- 1-- -30000.0
- 2-- -25000.0
- 3-- -20000.0
- 4-- -15000.0
- 5-- -10000.0
- 6-- -5000.0
- 7-- 0.0
- 8-- 5000.0
- 9-- 10000.0
- 10-- 15000.0
- 11-- 20000.0
- 12-- 25000.0

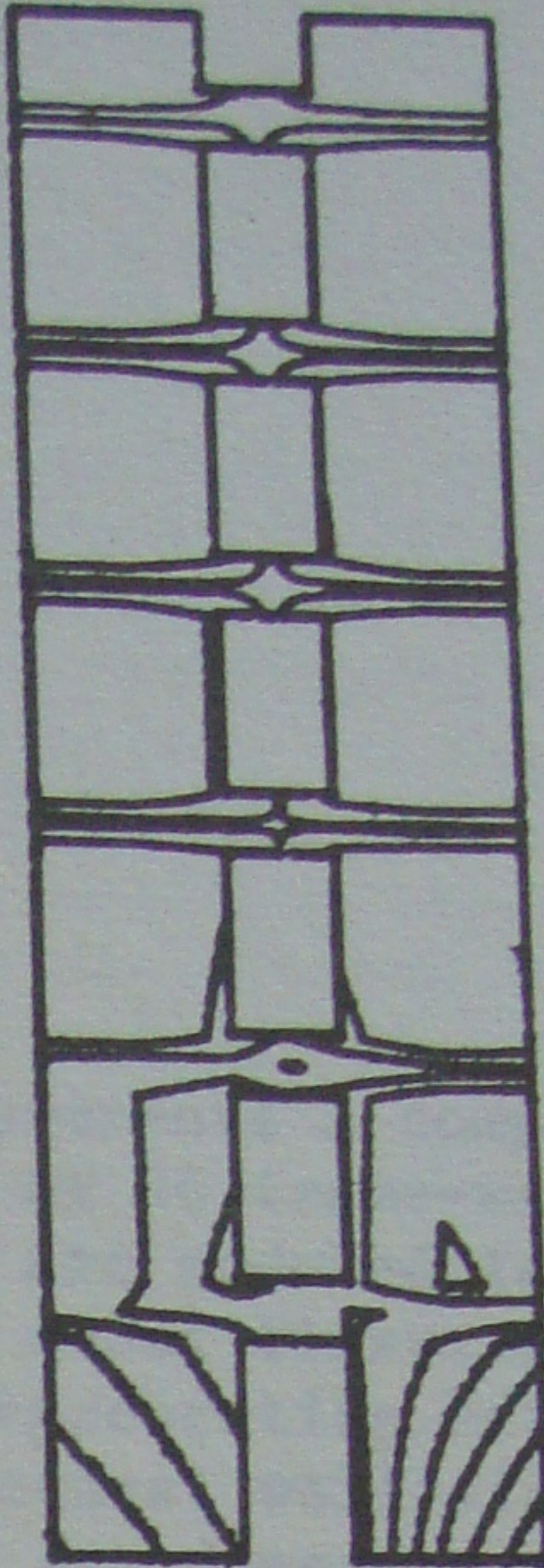
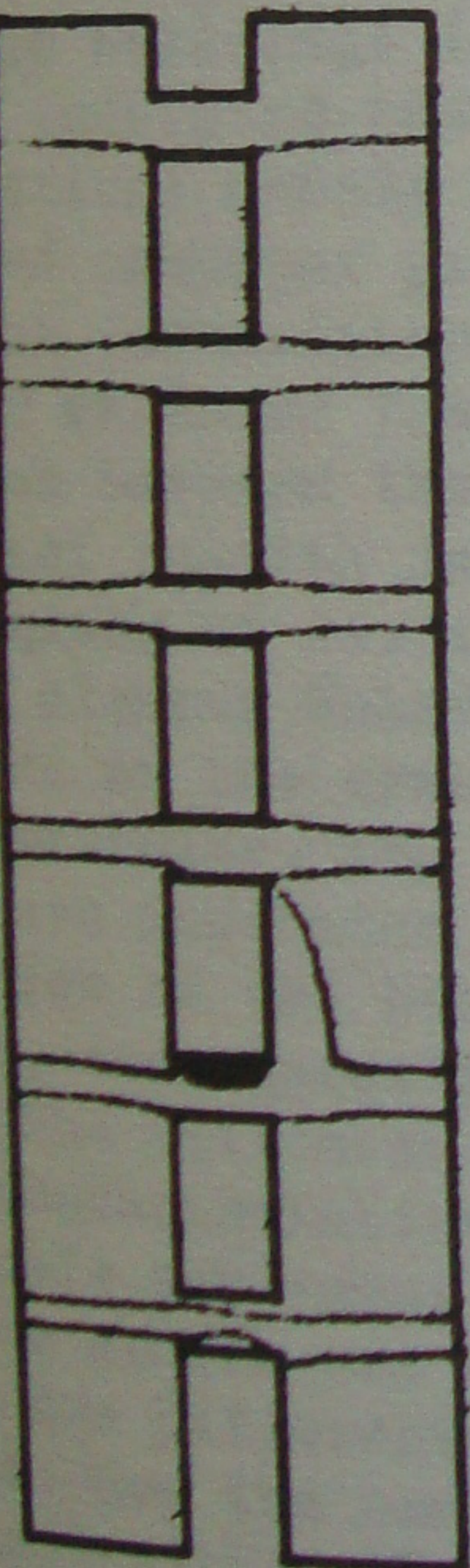


Fig. 10 WALL-1 at the 34th step of iteration

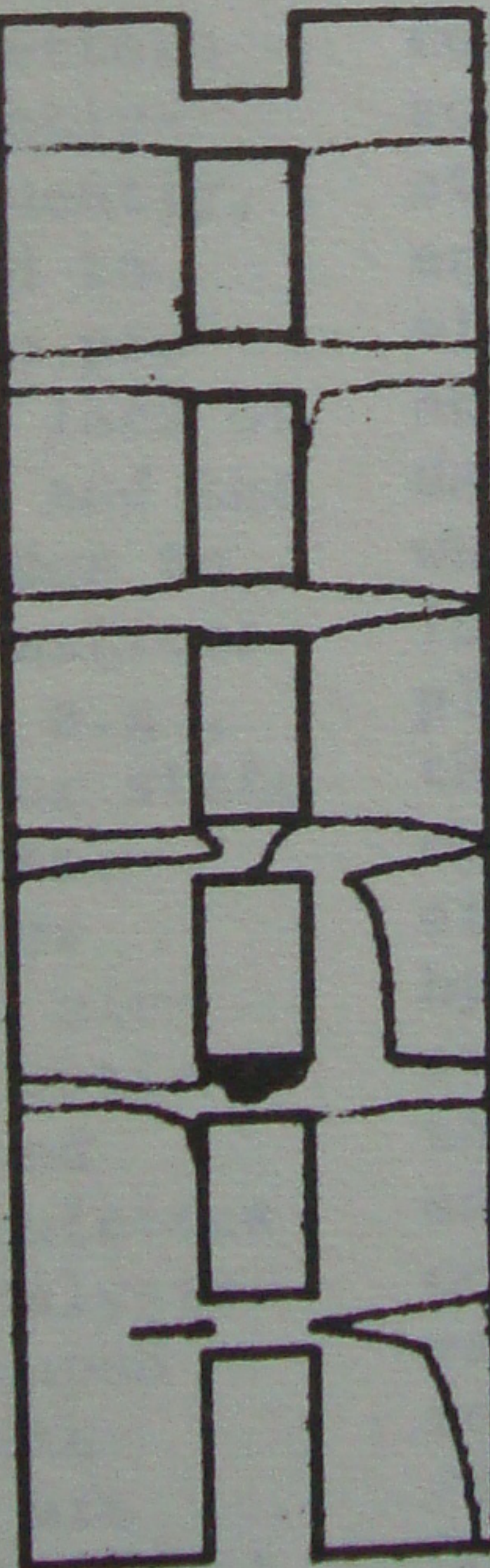
CONTOUR VALUES X STRESSES

- 1-- -100000.0
- 2-- -140000.0
- 3-- -180000.0
- 4-- -220000.0
- 5-- -260000.0
- 6-- -300000.0
- 7-- -340000.0
- 8-- -380000.0
- 9-- -420000.0
- 10-- -460000.0
- 11-- -50000.0



CONTOUR VALUES XY STRESSES

- 1-- -100000.0
- 2-- -140000.0
- 3-- -180000.0
- 4-- -220000.0
- 5-- -260000.0
- 6-- -300000.0
- 7-- -340000.0
- 8-- -380000.0
- 9-- -420000.0
- 10-- -460000.0
- 11-- -50000.0



CONTOUR VALUES MAXIMUM PRINCIPAL STRESSES

- 1-- -200000.0
- 2-- -240000.0
- 3-- -280000.0
- 4-- -320000.0
- 5-- -360000.0
- 6-- -400000.0
- 7-- -440000.0
- 8-- -480000.0
- 9-- -520000.0
- 10-- -560000.0
- 11-- -60000.0

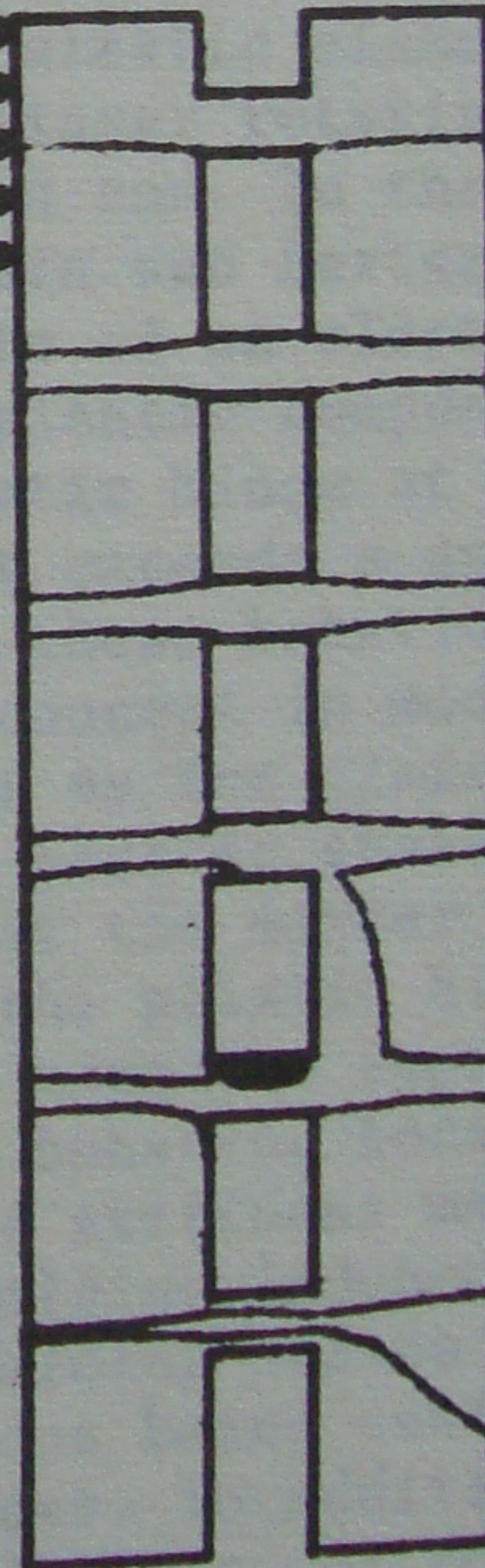


Fig. 11 WALL-1 at the 36th step of iteration